Cavity squeezing by a quantum conductor

Udson C Mendes, Christophe Mora

Cavity squeezing by a quantum conductor

2015 New J. Phys. 17 113014

(http://iopscience.iop.org/1367-2630/17/11/113014)

New Journal of Physics
The open access journal at the forefront of physics

Deutsche Physikalische Gesellschaft DPG
IOP Institute of Physics

Published in partnership with: Deutsche Physikalische Gesellschaft and the Institute of Physics

OPEN ACCESS

RECEIVED
27 May 2015

REVISED
31 August 2015

ACCEPTED FOR PUBLICATION
12 October 2015

PUBLISHED
3 November 2015

PAPER

Cavity squeezing by a quantum conductor

Udson C Mendes and Christophe Mora

Laboratoire Pierre Aigrain, École Normale Supérieure-PSL Research University, CNRS, Université Pierre et Marie Curie-Sorbonne Universités, Université Paris Diderot-Sorbonne Paris Cité, 24 rue Lhomond, F-75231 Paris Cedex 05, France

E-mail: mora@lpa.ens.fr

Keywords: circuit quantum electrodynamics, noise and electronic transport in nanoconductors, squeezed states of light, microwave emission, transport in quantum dots

Supplementary material for this article is available online

Abstract

Hybrid architectures integrating mesoscopic electronic conductors with resonant microwave cavities have a great potential for investigating unexplored regimes of electron–photon coupling. In this context, producing nonclassical squeezed light is a key step towards quantum communication with scalable solid-state devices. Here we show that parametric driving of the electronic conductor induces a squeezed steady state in the cavity. We find that squeezing properties of the cavity are essentially determined by the electronic noise correlators of the quantum conductor. In the case of a tunnel junction, we predict that squeezing is optimized by applying a time-periodic series of quantized δ—peaks in the bias voltage. For an asymmetric quantum dot, we show that a sharp Leviton pulse is able to achieve perfect cavity squeezing.

1. Introduction

Squeezed states of light [1] exhibit reduced noise below the vacuum level in one of their quadrature and amplification in the other quadrature. Their realization is a key step in the development of quantum communication. They are important tools for continuous variable quantum information protocols [2, 3] where they serve as building blocks for generating non-classical states. Their enhanced sensitivity can also be used for quantum non-demolition measurements of position and force [4]. Easily produced in optical systems, squeezed states have been observed more recently in circuit quantum electrodynamics at microwave frequencies [5], either as single-mode [6, 7], two-mode squeezing [8, 9] or as Einstein–Podolsky–Rosen states [10].

The parametric driving used so far in experiments is limited to a half-squeezed quadrature for a cavity mode because of the inevitable coupling to the external vacuum fluctuations [11]. This limit however does not apply to dissipative squeezing, in which one steers the environment to stabilize the cavity into a non-classical state. In this case, perfect squeezing can be achieved, at least in principle, with minimum uncertainty [12, 13].

A recent development in the field of superconducting quantum circuits is the realization of hybrid systems in which a quantum conductor is coupled to a microwave resonator. These systems offer an appealing platform for investigating fundamental matter–light interactions with an experimental control on both the electronic and photonic parts [14–18]. Experiments have been realized with metallic tunnel junctions connected to a resonating line [19], or with quantum dots, realized in carbon nanotubes, nanowires or two-dimensional electron gases [20–26] embedded in high-finesse coplanar cavities. The interplay of electron transport and emission of photons can lead to an electronic-induced lasing state in the cavity [27–30], and more generally produce bunched or antibunched photons [31–35], and nonclassicality in the light emitted by a quantum conductor [36, 37]. Squeezed light emitted by a tunnel junction was recently demonstrated experimentally in the absence of a cavity [38–40].

In this paper, we describe dissipative squeezing of a cavity mode coupled to an ac driven electronic reservoir. The system, depicted in figure 1, is a quantum conductor coupled to a microwave resonator. In addition, a classical bias voltage, with an oscillating part at twice the resonator frequency, is applied to the conductor. The conductor plays the role of a nonlinear environment: photons from the ac modulation are broken into pairs and

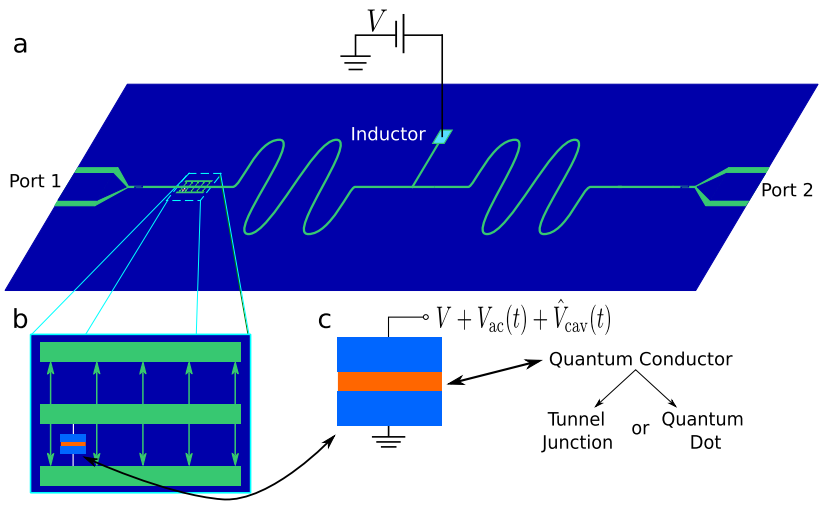

Figure 1. (a) Schematic of a resonant cavity realized in a superconducting transmission line. The center line is coupled to external electromagnetic modes (ports) via capacitive gaps delimiting the cavity. The output field of the cavity can be measured in these ports. A dc voltage can be applied to the center line at a voltage node in order to preserve the high-Q factor of the cavity [22, 41]. (b) Focus on the galvanic coupling between the cavity and a quantum conductor. The electric field (arrows) is spatially constant at the scale of the conductor. The conductor is lead-contacted on the upper side to the center line and on the lower side to the ground plane. (c) The quantum conductor can be a tunnel junction or a quantum dot. The upper lead is connected to the center line where the voltage potential is the sum of dc [V] and ac [$V_{ac}(t)$] parts, as well as the cavity quantum field $\propto a + a^{\dagger}$.

transmitted to the cavity, thereby producing squeezing. We show that the amount of cavity squeezing is determined solely by current noise fluctuations in the conductor. We focus our attention on ac excitations which optimizes squeezing. In the case of a tunnel junction, we find that the best solution consists of periodic and quantized voltage peaks occurring in phase with the compressed quadrature. We also discuss how squeezing improves with the number of harmonics in the ac signal. For a quantum dot, we identify the conditions of optimum squeezing: asymmetric coupling to the leads, a narrow single-level resonance, a far-detuned single-level energy and a dc bias voltage matching the resonator frequency. In addition, we show that a Leviton pulse results in a vacuum squeezed state with minimal uncertainty. Perfect squeezing is approached by narrowing the width of the voltage pulses in the Leviton, again in phase with the compressed quadrature.

2. Tunnel junction

We start by considering the case of a tunnel junction for the quantum conductor. The voltage bias across the junction is the sum of a driven classical part applied on the upper lead, and a quantum part associated to the cavity field. Using a convenient choice of electromagnetic gauge, it simply dresses the electron tunneling operators

$$H_{\mathrm{T}}(t) = \mathcal{T}\mathrm{e}^{-\mathrm{i}\hat{\varphi}(t)} + \mathcal{T}^{\dagger}\mathrm{e}^{\mathrm{i}\hat{\varphi}(t)}, \tag{1}$$

where the operator $\mathcal{T}$ transfers one electron from the upper to the lower lead while $\mathcal{T}^{\dagger}$ does the opposite [42, 43]. $\hat{\varphi}(t)$ is the total semi-classical phase accumulated during a tunneling event, decomposed as $\hat{\varphi}(t) = (eV/\hbar)t + \phi_{\mathrm{ac}}(t) + \mathrm{i}(g/\omega_0)(\hat{a}^{\dagger} - \hat{a})$, with the ac phase $\phi_{\mathrm{ac}}(t) = (e/\hbar)\int^{t} \mathrm{d}t'\, V_{\mathrm{ac}}(t')$. The last term is the quantum part and g measures the junction-cavity coupling strength. The cavity Hamiltonian is reduced for simplicity to a single mode, $H_{\mathrm{cav}} = \hbar\omega_0\hat{a}^{\dagger}\hat{a}$ with the cavity annihilation operator $\hat{a}$. Equation (1) contains both the excitation of the cavity state by electron tunneling events and photo-assisted transport phenomena triggered by the ac modulation [44, 45]. $H_T(t)$ is thus responsible for an exchange of energy between three sub-systems: the cavity, the ac classical field and lead (free) electrons.

We assume weak junction-cavity coupling and therefore neglect the backaction-induced change in electron tunneling resulting from the cavity. We thus set $g = 0$ to examine the current fluctuations of the tunnel junction and latter reinstate a finite g when considering the dynamics of the cavity field $\hat{a}$. In the presence of ac voltage modulation, the photo-assisted noise properties of the tunnel junction are characterized by the correlator (at $g = 0$) [46]

$$\left\langle \hat{I}(\omega_1)\hat{I}(\omega_2)\right\rangle = \sum_{n=-\infty}^{+\infty} S_n(\omega_1)2\pi\delta\left(\omega_1 + \omega_2 - 2n\omega_0\right), \tag{2}$$

where $\hat{I}(\omega)$ is the Fourier transform of the Heisenberg current operator $\hat{I}(t)$ of the junction. The $n=0$ term gives the stationary part of the noise, meaning that, when Fourier transformed with times t_1 and t_2, it depends only on the time difference $t_1 - t_2$ and not on the mean time $\bar{t} = (t_1 + t_2)/2$. $S_0(\omega)$ is called the absorption (emission) noise of the tunnel junction for $\omega > 0$ ($\omega < 0$) [47]. It governs the rate of energy transfer between the junction and its environment, here the cavity, via single photons of energy $\hbar|\omega|$.

As shown in the supplementary note 1, available at (stacks.iop.org/njp/17/113014/mmedia) the different noise terms can be calculated to leading order in the tunneling strength

$$2S_n(\omega) = \sum_{n'}\Big[c_{n'}c^*_{n'+n}\bar{S}\left(\omega + eV/\hbar + 2n'\omega_0\right) + c^*_{n'}c_{n'-n}\bar{S}\left(\omega - eV/\hbar - 2n'\omega_0\right)\Big]e^{-in\varphi}, \tag{3}$$

in terms of the (unsymmetrized) equilibrium Johnson–Nyquist noise of the tunnel junction $\bar{S}(\omega) = (2\omega/R_T)(1 - e^{-\hbar\omega/(k_BT)})^{-1}$, where R_T is the junction dc resistance. The coefficients c_m are defined by the Fourier expansion

$$e^{i\phi_{ac}(t)} = \sum_{m\in\mathbb{Z}} c_m e^{2im\omega_0 t}e^{im\varphi}, \tag{4}$$

of the ac phase ϕ_{ac}. φ is the overall phase of the ac signal. For the lead connected to the voltage $V_{ac}(t) = (\hbar/e)\dot{\phi}_{ac}(t)$, c_m gives the probability amplitude for an electron to absorb m energy quanta from the classical ac field when $m > 0$. $m < 0$ describes correspondingly photon emission to the ac field [48]. In the particular case of a sinusoidal excitation, $V_{ac}(t) = V_1\cos(2\omega_0 t + \varphi)$, these coefficients are written in terms of Bessel functions

$$c_m = J_m\left(\frac{eV_1}{2\hbar\omega_0}\right). \tag{5}$$

The energy of absorbed photons, $2m\hbar\omega_0$, can be either used in exciting energetic electron–hole pairs in the conductor, or transferred to the cavity. The non-stationary noise terms $S_{n\neq 0}$ in equation (2) oscillate with the mean time $\bar{t}$. They do not conserve energy and can provide n quanta of energy $2\hbar\omega_0$ (or absorb if $n < 0$) to the cavity. We will return below to the physical significance of these terms when analysing the cavity stationary state and squeezing effects.

Now that we have detailed the possible transfers of energy between the ac-excited tunnel junction and its environment (the cavity), we study the cavity evolution under the dissipative influence of the electrons. Assuming weak junction-cavity coupling, we expand H_T to first order in g/ω_0, $H_T = H_T^0 + i\lambda\hat{I}(\hat{a}^\dagger - \hat{a})$ with the coupling constant $\lambda = \hbar g/(e\omega_0)$. The cavity evolution is described by a Heisenberg–Langevin equation

$$\dot{\hat{a}} + i\omega_0\hat{a} + \frac{\kappa}{2}\hat{a} = \lambda\hat{I}(t), \tag{6}$$

justified, either by an input–output calculation [49] detailed in the supplementary note 2, or by a Keldysh path integral formulation, discussed in appendix B, assessing the Gaussian character of current and cavity field fluctuations. The tunnel junction current $\hat{I}(t)$ in equation (6) plays the role of a quantum noise term, with fluctuations characterized by the correlator of equation (2). In deriving this equation, we have neglected the intrinsic (bare) damping of the cavity κ_0, assuming that the cavity dissipation caused by the electrons dominates. The corresponding damping rate $\kappa = \lambda^2[S_0(\omega_0) - S_0(-\omega_0)]$ balances absorption and emission noises, since absorption (emission) noise corresponds to photon loss (gain) from the cavity. Our calculation is also based on the use of the rotating-wave approximation where rapidly oscillating terms are averaged to zero. The validity of this approximation is controlled by the smallness of κ/ω_0 and is consistent with our first order conductor-cavity coupling and with the absence of cavity backaction.

The first order differential equation (6) can be solved straightforwardly in time or frequency space, and yields the steady-state correlation functions for the cavity field $\hat{a}$. We find for the anomalous correlator, using that $\kappa \ll \omega_0$,

$$\left\langle\hat{a}^2\right\rangle = \frac{\lambda^2 S_1(\omega_0)}{\kappa} = \frac{S_1(\omega_0)}{S_0(\omega_0) - S_0(-\omega_0)}. \tag{7}$$

This result can be given a physical interpretation: $S_1(\omega_0)$ describes the coherent emission by the junction of a quantum of energy $2\hbar\omega_0$ to the cavity. This energy quantum breaks into a pair of cavity photons thereby contributing to the $\langle\hat{a}^2\rangle$ correlator. This effect is limited in the denominator by the rate at which cavity photons are absorbed by the tunnel junction. In the same way, the number of cavity photons $\langle\hat{a}^\dagger\hat{a}\rangle = \lambda^2 S_0(-\omega_0)/\kappa$ is unsurprisingly governed by the electronic emission noise.

We now investigate field squeezing more precisely and introduce the two quadratures $\hat{X}_1 = i(\hat{a}^\dagger e^{-i\varphi/2} - \hat{a}e^{i\varphi/2})$ and $\hat{X}_2 = \hat{a}^\dagger e^{-i\varphi/2} + \hat{a}e^{i\varphi/2}$, where we use the same phase φ as in equation (4). Their variance is readily obtained

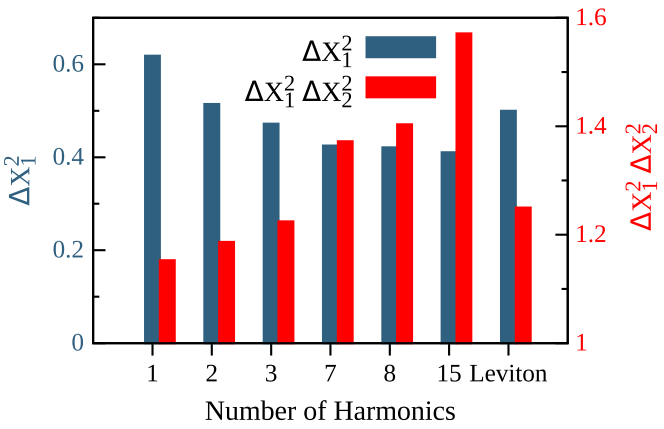

Figure 2. Minimum variance of the squeezed quadrature (left) and Heisenberg uncertainty product (right) as a function of the number of harmonics in the ac signal applied to a tunnel junction. The variance ΔX_1^2 of equation (8) is minimized numerically for the ac signal $V_{\rm ac}(t) = \sum_{j=1}^{n} V_j \cos(2j\omega_0 t)$ where n is the number of harmonics. Optimal squeezing is obtained with $T = 0$, $eV = \hbar\omega_0$. For comparison, the variance has been computed for a Leviton pulse with the result $\Delta X_1^2 = 1 - 2a + 2a^2$. The optimized Leviton with $a = 1/2$ is shown in the last column.

$$\Delta X_{1/2}^2 = \frac{\sum_n \left| c_n \mp c_{n+1} \right|^2 \bar{S}_e\left(eV/\hbar + (2n+1)\omega_0\right)}{\sum_n \left(\left| c_n \right|^2 - \left| c_{n+1} \right|^2 \right) \bar{S}_o\left(eV/\hbar + (2n+1)\omega_0\right)}, \tag{8}$$

where we introduced the even $\bar{S}_e$ and odd $\bar{S}_o$ parts of the Johnson-Nyquist noise $\bar{S}$. The two quadrature fluctuations are thus sensitive to the electronic temperature T, the dc bias voltage V and the pulse shape of the ac signal. The squeezing mechanism is optimized by taking the limit of vanishing temperature and by setting $eV = \hbar\omega_0$.

We first consider a single-tone driving of the tunnel junction, $V_{\rm ac}(t) = V_1 \cos(2\omega_0 t + \varphi)$, the experimentally most accessible situation. The photo-assisted coefficients c_n are then given by Bessel functions, as detailed in appendix A. A numerical minimization of ΔX_1^2 in equation (8) gives $\Delta X_1^2 = 0.618$ for $eV_1 = 0.706 \times 2\,\hbar\omega_0$, with $\Delta X_2^2 = 1.864$. This optimal squeezing value coincides exactly with the squeezing of the emitted light predicted and measured in [37, 38], see also the more recent [50]. This is explained by noting that the zero-temperature cavity damping $\kappa/\lambda^2 = 2\,\hbar\omega_0/R_T$ (the denominator in equation (8)) is constant for a tunnel junction, regardless of the bias voltage shape. This independence no longer holds at finite temperature or in the case of a conductor with a nonlinear I–V characteristic.

We turn to an ac modulation with the same fundamental frequency $2\,\omega_0$ but including higher harmonics [51]. Figure 2 shows the improvement in squeezing ΔX_1^2 by adding more and more harmonics while ΔX_2^2 is further amplified. Considering a general periodic signal, we find analytically, as shown in appendix C, that the minimum value $\Delta X_1^2 = 4/\pi^2 = 0.405$ is reached when $c_n = (1/\pi)(n + 1/2)^{-1}$ for $n \in \mathbb{Z}$, in agreement with a numerical minimization. The corresponding ac phase across the junction is a periodic piecewise linear function $\phi_{\rm ac}(t) = \pi/2 - \omega_0 t$ for $t \in]0,\ \pi/\omega_0[$, with a jump discontinuity of π at $t = 0$ and multiples of π/ω_0. Adding the dc voltage V, we find for the optimal voltage applied to the junction a series of δ-peaks

$$V_{\rm opt}(t) = \frac{h}{2e} \sum_{l \in \mathbb{Z}} \delta\left(t - \frac{l\pi}{\omega_0} \right). \tag{9}$$

It is useful to give an intuitive classical picture for this squeezing optimization: the bias potential $V_{\rm opt}(t)$ acts on the conductor specifically at times where the amplitude of the squeezed quadrature is maximum and the other quadrature vanishes. This is in fact a strong perturbation, the emission and absorption noises are infinite and the second variance $\Delta X_2^2 = +\infty$.

Despite its linear current response, the tunnel junction is able to squeeze the cavity state down to 40 % of the zero-point level. This is because squeezing is not governed by the current itself but by current fluctuations, and the noise of a tunnel junction is only a piecewise linear function enabling rectification [38]. Equation (8) nevertheless suggests that better squeezing can be achieved by using a genuine nonlinear system.

3. Asymmetric quantum dot

We consider a quantum dot for the conductor embedded in the cavity. The situation where the dot is symmetrically coupled to the two leads, discussed in the supplementary note 3, is not optimal for squeezing. We

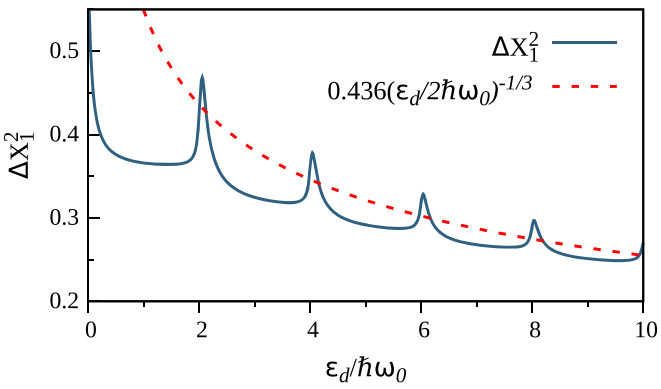

Figure 3. Squeezed variance for an asymmetric quantum dot driven by a single-tone excitation $V_{\rm ac}(t) = V_1\cos(2\omega_0 t + \varphi)$ versus the dot single-level energy, as given by equation (8) and equation (11). ΔX_1^2 is computed at $T = 0$, $eV = \hbar\omega_0$ and $\Gamma = 0.1\,\omega_0$. For each ε_d, V_1 is tuned to minimize ΔX_1^2. The first local minimum $\Delta X_1^2 = 0.358$ is reached for $\varepsilon_d = 1.54\,\hbar\omega_0$ and $eV_1/(2\hbar\omega_0) = 1.16$. Asymptotically at large ε_d, the minima follow the curve $0.436(\varepsilon_d/2\hbar\omega_0)^{-1/3}$ (in dotted line) and the optimal ac amplitude follows $eV_1 = \varepsilon_d$.

thus focus on the asymmetric case where the upper lead is more weakly coupled to the quantum dot than the lower lead. In this case, the voltage drop from the central strip to the ground mainly takes place at the upper dot-lead tunnel contact. The first order cavity-conductor coupling is then of the form $i\lambda\hat{I}_U(\hat{a}^\dagger - \hat{a})$ where $\hat{I}_U$ denotes the electrical current of electrons incoming from the upper lead. The coupling to the lower lead current is neglected.

In practice, for quantum dot geometries, it may be important to also take into account the coupling of electronic transport to phonons. Following [52] it would lead to tunneling processes involving the excitation of phonon–photon pairs, degrading the quality of squeezing. Such study is nevertheless beyond the scope of this work and we neglect electron-phonon coupling in what follows.

The analysis developed above for the tunnel junction can be essentially carried over to the quantum dot, with $\hat{I}_U$ replacing $\hat{I}$ in the Heisenberg–Langevin equation (6). The noise properties of the quantum dot are derived using scattering theory as discussed in appendix D. We retrieve noise factors similar to equation (3),

$$2S_n(\omega) = \sum_{n'}\Big[c_{n'}c^*_{n'+n}\bar{S}_+\big(\omega + eV/\hbar + 2n'\omega_0\big) + c^*_{n'}c_{n'-n}\bar{S}_-\big(\omega - eV/\hbar - 2n'\omega_0\big)\Big]e^{-in\varphi}, \tag{10}$$

here involving two different equilibrium noise terms

$$\bar{S}_\pm(\omega) = \frac{2e^2\Gamma_U\Gamma}{\pi\hbar^2}\int d\varepsilon \frac{f(\varepsilon - \hbar\omega)[1 - f(\varepsilon)]}{\big(\varepsilon \mp \varepsilon_d\big)^2 + (\hbar\Gamma/2)^2}, \tag{11}$$

with the Fermi function $f(\varepsilon) = (1 + e^{\varepsilon/k_BT})^{-1}$. The broadening Γ of the dot single energy level, denoted ε_d, can be decomposed according to its coupling to the upper and lower leads $\Gamma = \Gamma_U + \Gamma_L$ with $\Gamma_U \ll \Gamma_L$. The Lorentzian form in the integrand of equation (11) describes the Breit–Wigner resonance for transmitting electrons through the dot [53]. $\bar{S}_+(\omega)$ describes electron–hole excitations with energy $\hbar\omega$, where the electron, with energy ε, tunnels from the lower to the upper lead and has to meet the resonance condition of the dot single-level. $\bar{S}_-$ is the same but with hole tunneling. Proceeding with the calculation of cavity properties based on the Heisenberg–Langevin equation of motion, we retrieve the quadrature variances of equation (8) if we define the even/odd parts as $2\bar{S}_{e/o}(\omega) = \bar{S}_+(\omega) \pm \bar{S}_-(-\omega)$.

We have studied numerically the minimization of the variance ΔX_1^2. Quite generally, squeezing optimization requires zero temperature and the four-wave mixing condition $eV = \hbar\omega_0$ [38], as well as a sharp resonance, $\Gamma \ll \omega_0$. In this regime, for $\varepsilon_d > 0$, $\bar{S}_-$ becomes negligible and $\bar{S}_+$ in equation (8) is either constant for $n > n_{\rm th} = \varepsilon_d/(2\hbar\omega_0) - 1$, or vanishingly small below this threshold. $\bar{S}_e$ and $\bar{S}_o$ simplify in equation (8) and the summation involves only values of n above the threshold $n_{\rm th}$.

In the case of a single-frequency ac modulation, figure 3 shows that the squeezed variance ΔX_1^2 displays a series of local minima, where the values of the minima decrease with ε_d. Large single-level energy ε_d however implies stronger power in the ac excitation signal in order to meet the Breit–Wigner resonance condition. In practice, this requires an ac signal amplitude V_1 close to ε_d such that electrons can tunnel through the dot. Perfect squeezing $\Delta X_1^2 = 0$ is reached at very large ε_d but only with a weak power law of coefficient $-1/3$.

Alternatively, a vacuum squeezed state can be reached in the cavity by using a Leviton ac signal with the fundamental frequency $2\,\omega_0$. Leviton pulses were originally [54] proposed as voltage excitations designed to transfer a finite number of electrons through a coherent conductor with minimal noise, in analogy with coherent

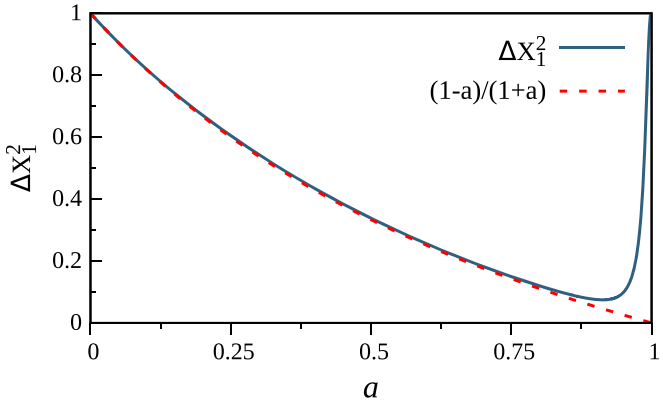

Figure 4. Squeezed variance for the asymmetric quantum dot as a function of the Leviton pulse excitation parameter a. The continuous line was computed using equations (8) and (11) at zero temperature, $eV = \hbar\omega_0, \Gamma/\omega_0 = 0.1$, $\varepsilon_d = 6\,\hbar\omega_0$ and the Leviton c_n coefficients (see appendix A). It is compared to the asymptotical expression $(1-a)/(1+a)$ (dotted line) valid for an infinitely sharp resonance $\Gamma \to 0$. Note that the limit $a = 1$ corresponds to a dc voltage $eV = -\hbar\omega_0$ producing no squeezing $\Delta X_1^2 = 1$, indicating that the limits $\Gamma/\omega_0 \to 0$ and $a \to 1$ do not commute.

states minimizing quantum-mechanical uncertainty. They consist of sums of Lorentzian pulses with unit flux each. A unit flux represents the attempt to transmit a single electron. Mathematical details are briefly reviewed in appendix A. A Leviton can be periodized by having an infinite train of evenly spaced Lorentzian pulses [48, 55]. Leviton pulses have recently been synthesized and used to perform Hong–Ou–Mandel electronic experiments [56] and electron quantum tomography [57].

The use of a Leviton pulse for squeezing is natural. A Leviton train with periodic short pulses addresses specifically one quadrature (the one to be squeezed), while producing a minimal disturbance (noise) on the quantum conductor. Taking the limit of a very sharp resonance $\Gamma/\omega_0 \to 0$ and the bias voltage $eV = \hbar\omega_0$, one obtains for the squeezed variance

$$\Delta X_1^2 = \frac{\sum_{n=0}^{\infty}\left(c_n - c_{n+1}\right)^2}{\sum_{n=0}^{\infty}\left(c_n^2 - c_{n+1}^2\right)} = \frac{1-a}{1+a}, \tag{12}$$

for $0 < \varepsilon_d < 2\hbar\omega_0$, and a minimal Heisenberg uncertainty $\Delta X_1\, \Delta X_2 = 1$ reflecting the minimized perturbation by the Leviton compared to other types of ac excitation. $a = \mathrm{e}^{-2\omega_0\tau}$ is a parameter related to the width τ of each Lorentzian pulse. A Leviton pulse is thus able to produce in optimal conditions an ideal squeezed state with arbitrary compression.

As shown in figure 4, squeezing saturates at finite damping Γ. For a reasonable damping rate $\Gamma/\omega_0 = 0.1$, we find that the squeezed variance can still be reduced down to $\Delta X_1^2 = 0.075$ for $a = 0.91$. A Leviton excitation with parameter a close to 1 exhibits sharp voltage pulses of width $\tau \simeq (1-a)/(2\,\omega_0)$. Similarly to the tunnel junction, it corresponds to concentrate short-time pulses of high voltage when the amplitude of the squeezed quadrature is maximum while the other quadrature vanishes.

4. Cavity readout

Cavity squeezing could be evidenced by an *in situ* measurement using a qubit and its anisotropic radiative decay [58]. It is also possible to demonstrate squeezing in the cavity by measuring the output field. So far, we have neglected in our discussion the coupling of the cavity to the external electromagnetic modes, see figure 1. They introduce an additional damping rate κ_0. As detailed in the supplementary note 2, this external damping adds two terms in the Heisenberg–Langevin equation (6), which now reads

$$\dot{\hat{a}} + \mathrm{i}\omega_0\hat{a} + \frac{\kappa + \kappa_0}{2}\hat{a} = -\sqrt{\kappa_0}\;\hat{b}_{\mathrm{in}}(t) + \lambda\hat{I}(t). \tag{13}$$

$\hat{b}_{\mathrm{in}}(t)$ is the input field, it describes the quantum state of incident photons on the cavity. In the absence of an input drive, it corresponds to vacuum noise with $\langle\hat{b}_{\mathrm{in}}(t)\hat{b}_{\mathrm{in}}{}^{\dagger}(t')\rangle = \delta(t-t')$ at zero temperature. The output field, describing photons escaping the cavity, is given by $\hat{b}_{\mathrm{out}} = \hat{b}_{\mathrm{in}} + \sqrt{\kappa_0}\;\hat{a}$ and obtained by solving equation (13).

Squeezing properties of the cavity are revealed by homodyne detection of the output field [5, 6], mixing it with a local oscillator with the cavity frequency ω_0 and phase θ. The power spectrum $S_D(\omega)$ [59] of the

homodyne detector signal $\hat{I}_D(t) \propto \hat{b}_{\rm out}(t)e^{i(\omega_0 t+\theta)} + {\rm h.c.}$ exhibits a deep at zero frequency and $\theta = \pi/2 + \varphi/2$, where the squeezing effect is most visible, with

$$\frac{S_D(\omega=0)}{S_D^0} = 1 + \frac{4\kappa_0}{\kappa}\left(\Delta X_1^2 - 1\right) < 1, \tag{14}$$

assuming weak external damping $\kappa_0 \ll \kappa$. S_D^0 denotes the vacuum level, measured in the absence of ac excitation. A value smaller than one in this equation indicates a squeezed output field. Interestingly, output squeezing is weak in this limit due to pollution by the input vacuum noise. As discussed in appendix E, the output field gets more squeezed as κ_0 increases, the best squeezing being obtained for equal external and electronic dampings. This is however at the price of weaker squeezing in the cavity. Perfect squeezing could even be reached in the output field, limiting in this case the cavity state to half-squeezing.

5. Conclusion and outlook

We studied the squeezing generated in a resonant cavity by coupling it to a mesoscopic conductor under parametric excitation. We showed that the quality of squeezing can be improved by enhancing nonlinearities in the conductor and by concentrating the voltage excitation pulses at instants where the squeezed quadrature amplitude reaches its maximum. In optimal conditions, perfect squeezing can even be achieved. We remark that nonlinearities could also be enhanced in a tunnel junction by increasing the coupling to the cavity and the associated dynamical Coulomb blockade [60]. More generally, our results can be easily extended to other quantum conductors for which the photo-assisted noise spectra are known or can be computed. They also suggest the possibility to engineer squeezed light for quantum information using electronic quantum conductors.

Acknowledgments

We thank C Altimiras, B Huard, P Joyez, F Mallet, F Portier, P Simon and M Trif for fruitful discussions. UCM acknowledges the support from CNPq-Brazil (Project No. 229659/2013-6).

Appendix A. Leviton excitation

A Leviton is a pulse shape designed to minimize shot noise in driving electric current [54]. In its periodized form, the time-dependent voltage is given by a sum of quantized Lorentzian pulses

$$V_{\rm ac}(t) = -2\hbar\omega_0 + \frac{h}{e}\sum_{l\in\mathbb{Z}}\frac{1}{\pi}\frac{\tau}{\tau^2 + \left(t - l\pi/\omega_0\right)^2}, \tag{A.1}$$

of common width τ. The ac phase is obtained by time-integration, $\phi_{\rm ac}(t) = (e/\hbar)\int^t {\rm d}t' V_{\rm ac}(t')$. It is conveniently written using the cyclic variable $z = e^{2i\omega_0 t}$, namely after a few algebraic manipulation [55]

$$e^{i\phi_{\rm ac}} = \frac{1}{z}\frac{z-a}{1-az} \tag{A.2}$$

where $0 < a = e^{-2\omega_0\tau} < 1$ is related to the pulses width. The conventional Leviton pulse, shaped to minimize zero-frequency shot noise, has the dc level $eV = 2\hbar\omega_0$, cancelling the first term in equation (A.1). In the main text, the dc bias chosen to optimize squeezing is $eV = \hbar\omega_0$. It can be understood by noting that the goal here is to minimize finite frequency noise correlators at the frequency ω_0. Expanding equation (A.2) in powers of z, we obtain $c_{-1} = -a$, $c_{n\geqslant 0} = a^n(1-a^2)$: there is a strong imbalance between absorption and emission of photons. $a = 1$ is no longer an ac modulation but corresponds to a shift of the dc voltage by $-2(\hbar/e)\omega_0$.

Appendix B. Keldysh formulation and Heisenberg–Langevin equation

The out-of-equilibrium physics of our system is conveniently described within the Keldysh path-integral formalism [61], enabling a systematic integration of the electronic degrees of freedom and yielding an effective action for the photons [62]. The action obtained, equations (B.3) and (B.4), can be shown to be equivalent to the Heisenberg–Langevin equation of motion equation (6) used in the main text, in the limit of small $\kappa/\omega_0 \ll 1$. For a direct derivation of the Heisenberg–Langevin equation in the spirit of input–output theory, see supplementary note 2.

The partition function (hereafter $\hbar = 1$)

$$\mathcal{Z} = \int \mathcal{D}\left[a,\, a^*\right] e^{iS_{cav}} \int \mathcal{D}\left[c,\, c^*\right] e^{i\left(S_e + S_{ep}\right)} \tag{B.1}$$

involves an integration over complex-valued fields, a,a^* for photons and c,c^* for electrons. S_e is the action for the isolated conductor, S_{cav} the photonic part corresponding to the Hamiltonian $H_{cav} = \hbar\omega_0 \hat{a}^\dagger \hat{a}$ and the electron–photon coupling is to first order

$$S_{ep} = -\frac{i\lambda}{\sqrt{2}} \int_{-\infty}^{+\infty} dt \sum_{\eta \pm 1} \eta\, I_\eta(t) \left(a_\eta^*(t) - a_\eta(t)\right), \tag{B.2}$$

where η denotes the Keldysh time branch. I is the quantum conductor current written with complex-valued fields.

The electronic part can be rigorously integrated using the cumulant expansion $\left\langle e^{iS_{ep}}\right\rangle_e = e^{i\left\langle S_{ep}\right\rangle_e - (1/2)\left\langle \delta S_{ep}{}^2\right\rangle_e + \cdots}$, where we use the notations $\delta S_{ep} = S_{ep} - \langle S_{ep}\rangle$ and $\int \mathcal{D}[c,\, c^*] e^{iS_e} A = \langle A\rangle_e$. We assume $\langle S_{ep}\rangle_e = 0$, a finite $\langle S_{ep}\rangle_e$ can be absorbed by a small shift $\propto g$ in the cavity fields. To summarize, we square S_{ep}, take its quantum average restricted to electronic degrees of freedom, and thus obtain a self-energy kernel for the photons involving current noise correlators. For clarity, we switch to classical/quantum variables, $a_{cl}/q = (a + \pm a_-)/\sqrt{2}$ and write the action in frequency space in order to take advantage of the current noise correlators given in equation (2). Summing S_{cav} and $(i/2)\langle S_{ep}^2\rangle_e$, we find the effective action

$$S_{eff} = \int_\omega \begin{pmatrix} a_{cl}^* & a_q^* \end{pmatrix} \begin{pmatrix} 0 & G_A^{-1}(\omega) \\ G_R^{-1}(\omega) & -\Sigma_K \end{pmatrix} \begin{pmatrix} a_{cl} \\ a_q \end{pmatrix} + S_a, \tag{B.3}$$

where we used the notation $\int_\omega = \int_{-\infty}^{+\infty} \frac{d\omega}{2\pi}$, and $a_{cl}(t) = \int_\omega a_{cl}(\omega) e^{-i\omega t}$. The retarded photon Green's function $G_R^{-1}(\omega) = \omega - \omega_0 + i\kappa/2$ has a pole shifted by half the damping rate κ (see main text). The quantum-quantum self-energy part is $\Sigma_K = -i\lambda^2 [S_0(\omega_0) + S_0(-\omega_0)]$. The effective action S_{eff} includes also an anomalous term, responsible for state squeezing

$$S_a = -i\lambda^2 \int_\omega \left(a_q^*(\omega) a_q^*\left(2\omega_0 - \omega\right) S_1(\omega_0) + \text{c.c.}\right). \tag{B.4}$$

Note that the real part of the self-energy induces in general a cavity pull which has been absorbed into a redefinition of ω_0. Computing this frequency shift consistently requires the second order term in the expansion of H_T in powers of g/ω_0, namely

$$\delta S_{ep}^{(2)} = -\frac{e^2\lambda^2}{2} \int_{-\infty}^{+\infty} dt \sum_{\eta \pm 1} \eta\, V_{T,\eta}(t) \left[a_\eta^*(t) - a_\eta(t)\right]^2, \tag{B.5}$$

where $V_T = \mathcal{T} + \mathcal{T}^\dagger$. The cavity frequency shift then vanishes for a tunnel junction.

The derivation of equations (B.3) and (B.4) relies on the rotating-wave approximation, valid for $\kappa \ll \omega_0$, where the fields $a_{cl/q}(\omega)$, $a_{cl/q}^*(\omega)$ take significant values only for $\omega \simeq \omega_0$. In principle, the anomalous part of the action S_a also contains terms with $a_{cl}(\omega)\, a_q(2\omega_0 - \omega)$, corresponding to the effect of non-stationary noise terms on the damping. Those terms are found to be proportional to $S_1(\omega) - S_1(2\omega_0 - \omega)$ and thus vanish for $\omega \simeq \omega_0$, with the small parameter κ/ω_0.

Finally, we discuss the connexion between the quadratic action of equation (B.3) and the Heisenberg–Langevin equation (6). Quite generally, it is known that current fluctuations in a tunnel junction, or a quantum conductor, are not gaussian. Nevertheless, computing the non-gaussian current contributions to the statistics of photons, one finds that they are small compared to the dominant Wick-like contractions among the current operators. This is true in the limit of weak damping, $\kappa \ll \omega_0$, where cavity correlation functions only involve current operators $\hat{I}$ at frequencies $\pm\omega_0$. For example, the fourth-order cavity field correlator gives, for $|t_i| \ll 1/\omega_0$,

$$\left\langle \hat{a}_{t_1}^{(\dagger)} \hat{a}_{t_2}^{(\dagger)} \hat{a}_{t_3}^{(\dagger)} \hat{a}_{t_4}^{(\dagger)} \right\rangle = \left(\sum_{P \in \mathbb{S}_4} \left\langle \hat{a}_{t_{P(1)}}^{(\dagger)} \hat{a}_{t_{P(2)}}^{(\dagger)} \right\rangle \left\langle \hat{a}_{t_{P(3)}}^{(\dagger)} \hat{a}_{t_{P(4)}}^{(\dagger)} \right\rangle \right) \left(1 + \mathcal{O}\left(\frac{\kappa}{\max\left(\left| eV/\hbar - \omega_0 \right|,\, eV_{ac}/\hbar \right)} \right) \right), \tag{B.6}$$

implying photon gaussian statistics except for the specific case of eV close to $\hbar\omega_0$ with no ac excitation. A related discussion can be found in [31, 32]. The reason is that an electron–hole excitation with energy $\hbar\omega_0$ created by a current operator $\hat{I}_{\omega_0}$ must be destroyed by another single current operator, the phase-space for alternative processes-where electron and hole are annihilated by two distinct current operators-being negligible for weak damping κ. This argument pertains to higher-order correlation functions such that, for the purpose of photon statistics, it is legitimate to keep only the gaussian part of electronic current fluctuations. The resulting cavity field statistics are obviously gaussian.

The above cumulant expansion can be rigorously stopped after the second order and the gaussian action in equation (B.3) becomes exact as long as κ is negligible with respect to ω_0. Computing second-order cavity correlations functions, with different ordering of $\hat{a}$ and $\hat{a}^\dagger$, we find coinciding results for the gaussian action and the Heisenberg–Langevin evolution. This completes the proof of the equivalence of the two formulations. This comparison differs from the standard derivation of a classical Langevin equation using the Keldysh action [63], in which case information about operator ordering is lost.

Appendix C. Optimized squeezing for a tunnel junction

In this section, we set $\hbar = 1$ for simplicity. We focus on the zero-temperature case, relevant to maximize the cavity state compression. In this case

$$\bar{S}_o\Big[eV + (2n+1)\omega_0\Big] = \frac{1}{R_T}\Big[eV + (2n+1)\omega_0\Big] \tag{C.1}$$

and the denominator in equation (8) of the main text simplifies to

$$\sum_{n\in\mathbb{Z}}\Big(\big|c_n\big|^2 - \big|c_{n+1}\big|^2\Big)\Big(eV + (2n+1)\omega_0\Big) = 2\omega_0, \tag{C.2}$$

regardless of V and the c_n coefficients. At the optimal dc voltage $eV = \hbar\omega_0$, the squeezed variance takes the simple form

$$\Delta X_1^2 = \sum_{n\in\mathbb{Z}}\big|c_n \pm c_{n-1}\big|^2|n|, \tag{C.3}$$

which we still need to minimize with respect to the distribution of Fourier coefficients c_n,

$$c_n = \frac{\omega_0}{\pi}\int_0^{\pi/\omega_0} \mathrm{d}t\ \mathrm{e}^{\mathrm{i}\phi_{\mathrm{ac}}(t)}\mathrm{e}^{-2\mathrm{i}n\omega_0 t}. \tag{C.4}$$

We now prove that the pulse shape of equation (9) in the main text, corresponding to the piecewise linear phase $\phi_{\mathrm{ac,opt}}(t) = \pi/2 - \omega_0 t$, extremizes the variance ΔX_1^2. We first differentiate equation (C.4) to obtain

$$\frac{\partial c_n}{\partial\phi_{\mathrm{ac}}(t)} = \frac{\mathrm{i}\omega_0}{\pi}\mathrm{e}^{\mathrm{i}\phi_{\mathrm{ac}}(t)}\mathrm{e}^{-2\mathrm{i}n\omega_0 t}, \tag{C.5}$$

which gives $-(\omega_0/\pi)\mathrm{e}^{-\mathrm{i}(2n+1)\omega_0 t}$ when evaluated at $\phi_{\mathrm{ac,opt}}(t)$. Using this result, we can proceed with the derivative of ΔX_1^2 with respect to an arbitrary form of $\phi_{\mathrm{ac}}(t)$

$$\frac{\partial\Delta X_1^2}{\partial\phi_{\mathrm{ac}}(t)} = 2\sum_n |n|\mathrm{Re}\Big[\Big(c_n^* - c_{n-1}^*\Big)\Big(\partial_{\phi_{\mathrm{ac}}}c_n - \partial_{\phi_{\mathrm{ac}}}c_{n-1}\Big)\Big]. \tag{C.6}$$

We evaluate this derivative with $\phi_{\mathrm{ac,opt}}(t)$ and its coefficients

$$c_n = \frac{1}{\pi}\frac{1}{n+1/2}, \tag{C.7}$$

and obtain

$$\frac{\partial\Delta X_1^2}{\partial\phi_{\mathrm{ac}}(t)} = \frac{2\omega_0}{\pi}\,\mathrm{Re}\left[\sum_{n\in\mathbb{Z}}\frac{|n|}{(n+1/2)(n-1/2)}\Big(\mathrm{e}^{-\mathrm{i}(2n+1)\omega_0 t} - \mathrm{e}^{-\mathrm{i}(2n-1)\omega_0 t}\Big)\right] = 0, \tag{C.8}$$

which completes the proof.

Inserting the coefficients equation (C.7) into the quadrature variance equation (C.3), we find

$$\Delta X_1^2 = \sum_{n\in\mathbb{Z}}\frac{|n|}{\pi^2(n+1/2)^2(n-1/2)^2} = \frac{4}{\pi^2}. \tag{C.9}$$

We also checked numerically that $\phi_{\mathrm{ac,opt}}(t)$ reaches the global minimum of ΔX_1^2.

Appendix D. Landauer–Büttiker calculation of the noise

The noise properties of the quantum dot are derived using the scattering, or Landauer–Büttiker, formalism [64]. The current operator is expanded over the basis of one-particle scattering states originating from both leads. The general case is reviewed in the supplementary note 4, we focus here on the asymmetric case where the probability for single-electron transmission at resonance $4\Gamma_U/\Gamma \ll 1$ is small, and expressions simplify. Omitting spin, the current operator has the form

$$\hat{I}_U(t) = \frac{ie\sqrt{\Gamma_U\Gamma}}{h}\int\int d\varepsilon_1 d\varepsilon_2\, \hat{c}_U^\dagger(\varepsilon_1) g(\varepsilon_2)\hat{c}_L(\varepsilon_2) \times e^{i\left[(\varepsilon_1-\varepsilon_2+V)t/\hbar+\phi_{ac}(t)\right]} + \text{h.c.} \quad (D.1)$$

with the Breit–Wigner resonant function $g(\varepsilon) = (\varepsilon - \varepsilon_d + i\hbar\Gamma/2)^{-1}$. The operator $\hat{c}_{U/L}(\varepsilon)$ annihilates an electron in a scattering state of energy ε incoming from the upper/lower lead. The normalization is fixed by the average

$$\left\langle \hat{c}_\alpha^\dagger(\varepsilon)\hat{c}_{\alpha'}(\varepsilon')\right\rangle = \delta_{\alpha,\alpha'} f(\varepsilon)\delta(\varepsilon - \varepsilon') \quad (D.2)$$

with the Fermi function $f(\varepsilon) = (1 + e^{\varepsilon/k_BT})^{-1}$. Due to the small capacitance at the upper dot-lead contact, the dc and ac bias voltages are applied essentially across this tunnel contact, the voltage potentials on both the quantum dot and the lower lead are fixed to the ground. Apart from the Breit–Wigner function, the rest of the calculation is similar to the case of a tunnel junction. The two-current correlators have the form of equation (2) and equation (3), where the equilibrium noise terms are given equation (11) in the main text.

Appendix E. Finite external damping

We briefly discuss the case of a bare cavity damping κ_0 comparable to the electronic damping κ, but still much smaller than the resonator frequency ω_0. The complete Heisenberg–Langevin equation (13) is solved by considering both the input field and electronic current fluctuations. One obtains for the two cavity field quadratures

$$\Delta X_{1/2}^2(\kappa_0) = 1 + \frac{\kappa}{\kappa+\kappa_0}\left(\Delta X_{1/2}^2(0) - 1\right), \quad (E.1)$$

where

$$\Delta X_{1/2}^2(0) = \frac{S_0(\omega_0) + S_0(-\omega_0) \mp 2\,\mathrm{Re}\left[S_1(\omega_0)\right]}{S_0(\omega_0) - S_0(-\omega_0)} \quad (E.2)$$

denote their variances in the absence of intrinsic damping κ_0, also given by equation (8) and discussed in length in the main text. Additionally, one finds for the output field squeezing, characterized by the power spectrum

$$\frac{S_D(\omega=0)}{S_D^0} = 1 + \frac{4\kappa_0\kappa}{(\kappa+\kappa_0)^2}\left(\Delta X_1^2(0) - 1\right). \quad (E.3)$$

Whereas a vanishing $\Delta X_1^2(0)$ clearly optimizes squeezing in both the cavity and output fields, there is no such choice for κ_0. Increasing κ_0 from zero improves squeezing in the output field but degrades cavity squeezing. Perfect squeezing in the output field is reached for $\kappa = \kappa_0$, with vanishing $\Delta X_1^2(0)$, in which case the cavity field is only half-squeezed.

References

[1] Walls D F 1983 Squeezed states of light *Nature* **306** 141–6
[2] Braunstein S L and Loock P v 2005 Quantum information with continuous variables *Rev. Mod. Phys.* **77** 513–77
[3] Menzel E P *et al* 2012 Path entanglement of continuous-variable quantum microwaves *Phys. Rev. Lett.* **109** 250502
[4] Caves C M, Thorne K S, Drever R W P, Sandberg V D and Zimmermann M 1980 On the measurement of a weak classical force coupled to a quantum-mechanical oscillator: I. Issues of principle *Rev. Mod. Phys.* **52** 341–92
[5] Yurke B, Kaminsky P G, Miller R E, Whittaker E A, Smith A D, Silver A H and Simon R W 1988 Observation of 4.2-k equilibrium-noise squeezing via a Josephson-parametric amplifier *Phys. Rev. Lett.* **60** 764–7
[6] Castellanos-Beltran M A, Irwin K D, Hilton G C, Vale L R and Lehnert K W 2008 Amplification and squeezing of quantum noise with a tunable josephson metamaterial *Nat. Phys.* **4** 929–31
[7] Mallet F, Castellanos-Beltran M A, Ku H S, Glancy S, Knill E, Irwin K D, Hilton G C, Vale L R and Lehnert K W 2011 Quantum state tomography of an itinerant squeezed microwave field *Phys. Rev. Lett.* **106** 220502
[8] Eichler C, Bozyigit D, Lang C, Baur M, Steffen L, Fink J M, Filipp S and Wallraff A 2011 Observation of two-mode squeezing in the microwave frequency domain *Phys. Rev. Lett.* **107** 113601
[9] Wilson C M, Johansson G, Pourkabirian A, Simoen M, Johansson J R, Duty T, Nori F and Delsing P 2011 Observation of the dynamical casimir effect in a superconducting circuit *Nature* **479** 376–9
[10] Flurin E, Roch N, Mallet F, Devoret M H and Huard B 2012 Generating entangled microwave radiation over two transmission lines *Phys. Rev. Lett.* **109** 183901
[11] Milburn G and Walls D F 1981 Production of squeezed states in a degenerate parametric amplifier *Opt. Commun.* **39** 401–4
[12] Kronwald A, Marquardt F and Clerk A A 2013 Arbitrarily large steady-state bosonic squeezing via dissipation *Phys. Rev.* A **88** 063833
[13] Didier N, Qassemi F and Blais A 2014 Perfect squeezing by damping modulation in circuit quantum electrodynamics *Phys. Rev.* A **89** 013820
[14] Cottet A, Mora C and Kontos T 2011 Mesoscopic admittance of a double quantum dot *Phys. Rev.* B **83** 121311

[15] Bergenfeldt C and Samuelsson P 2012 Microwave quantum optics and electron transport through a metallic dot strongly coupled to a transmission line cavity *Phys. Rev.* B **85** 045446
[16] Souquet J-R, Woolley M J, Gabelli J, Simon P and Clerk A A 2014 Photon-assisted tunneling with non-classical light *Nat. Commun.* **5** 5562
[17] Schiró M and Hur K Le 2014 Tunable hybrid quantum electrodynamics from nonlinear electron transport *Phys. Rev.* B **89** 195127
[18] Cottet A, Kontos T and Douçot B 2015 Electron–photon coupling in mesoscopic quantum electrodynamics *Phys. Rev.* B **91** 205417
[19] Altimiras C, Parlavecchio O, Joyez P, Vion D, Roche P, Esteve D and Portier F 2014 Dynamical Coulomb blockade of shot noise *Phys. Rev. Lett.* **112** 236803
[20] Delbecq M R, Schmitt V, Parmentier F D, Roch N, Viennot J J, Fève G, Huard B, Mora C, Cottet A and Kontos T 2011 Coupling a quantum dot, fermionic leads, and a microwave cavity on a chip *Phys. Rev. Lett.* **107** 256804
[21] Delbecq M R, Bruhat L E, Viennot J J, Datta S, Cottet A and Kontos T 2013 Photon-mediated interaction between distant quantum dot circuits *Nat. commun.* **4** 1400
[22] Petersson K D, McFaul L W, Schroer M D, Jung M, Taylor J M, Houck A A and Petta J R 2012 Circuit quantum electrodynamics with a spin qubit *Nature* **490** 380
[23] Frey T, Leek P J, Beck M, Blais A, Ihn T, Ensslin K and Wallraff A 2012 Dipole coupling of a double quantum dot to a microwave resonator *Phys. Rev. Lett.* **108** 046807
[24] Basset J, Jarausch D-D, Stockklauser A, Frey T, Reichl C, Wegscheider W, Ihn T M, Ensslin K and Wallraff A 2013 Single-electron double quantum dot dipole-coupled to a single photonic mode *Phys. Rev.* B **88** 125312
[25] Viennot J J, Delbecq M R, Dartiailh M C, Cottet A and Kontos T 2014 Out-of-equilibrium charge dynamics in a hybrid circuit quantum electrodynamics architecture *Phys. Rev.* B **89** 165404
[26] Liu Y-Y, Petersson K D, Stehlik J, Taylor J M and Petta J R 2014 Photon emission from a cavity-coupled double quantum dot *Phys. Rev. Lett.* **113** 036801
[27] Jin P-Q, Marthaler M, Cole J H, Shnirman A and Schön G 2011 Lasing and transport in a quantum-dot resonator circuit *Phys. Rev.* B **84** 035322
[28] Xu C and Vavilov M G 2013 Full counting statistics of photons emitted by a double quantum dot *Phys. Rev.* B **88** 195307
[29] Kulkarni M, Cotlet O and Türeci H E 2014 Cavity-coupled double-quantum dot at finite bias: analogy with lasers and beyond *Phys. Rev.* B **90** 125402
[30] Liu Y-Y, Stehlik J, Eichler C, Gullans M J, Taylor J M and Petta J R 2015 Semiconductor double quantum dot micromaser *Science* **347** 285–7
[31] Beenakker C W J and Schomerus H 2001 Counting statistics of photons produced by electronic shot noise *Phys. Rev. Lett.* **86** 700–3
[32] Beenakker C W J and Schomerus H 2004 Antibunched photons emitted by a quantum point contact out of equilibrium *Phys. Rev. Lett.* **93** 096801
[33] Gabelli J, Reydellet L-H, Fève G, Berroir J-M, Plaçais B, Roche P and Glattli D C 2004 Hanbury brown-twiss correlations to probe the population statistics of GHZ photons emitted by conductors *Phys. Rev. Lett.* **93** 056801
[34] Lebedev A V, Lesovik G B and Blatter G 2010 Statistics of radiation emitted from a quantum point contact *Phys. Rev.* B **81** 155421
[35] Jin J, Marthaler M and Schön G 2015 Electroluminescence and multiphoton effects in a resonator driven by a tunnel junction *Phys. Rev.* B **91** 085421
[36] Cottet A, Kontos T and Douçot B 2013 Squeezing light with majorana fermions *Phys. Rev.* B **88** 195415
[37] Bednorz A, Bruder C, Reulet B and Belzig W 2013 Nonsymmetrized correlations in quantum noninvasive measurements *Phys. Rev. Lett.* **110** 250404
[38] Gasse G, Lupien C and Reulet B 2013 Observation of squeezing in the electron quantum shot noise of a tunnel junction *Phys. Rev. Lett.* **111** 136601
[39] Forgues J-C, Lupien C and Reulet B 2014 Emission of microwave photon pairs by a tunnel junction *Phys. Rev. Lett.* **113** 043602
[40] Forgues J-C, Lupien C and Reulet B 2015 Experimental violation of bell-like inequalities by electronic shot noise *Phys. Rev. Lett.* **114** 130403
[41] Chen F, Li J, Armour A D, Brahimi E, Stettenheim J, Sirois A J, Simmonds R W, Blencowe M P and Rimberg A J 2014 Realization of a single-cooper-pair Josephson laser *Phys. Rev.* B **90** 020506
[42] Safi I and Sukhorukov E V 2010 Determination of tunneling charge via current measurements *Europhys. Lett.* **91** 67008
[43] Safi I 2015 Time-dependent transport in arbitrary extended driven tunnel junctions (arXiv:1401.5950)
[44] Tien P K and Gordon J P 1963 Multiphoton process observed in the interaction of microwave fields with the tunneling between superconductor films *Phys. Rev.* **129** 647–51
[45] Kouwenhoven L P, Jauhar S, Orenstein J, McEuen P L, Nagamune Y, Motohisa J and Sakaki H 1994 Observation of photon-assisted tunneling through a quantum dot *Phys. Rev. Lett.* **73** 3443–6
[46] Gabelli J and Reulet B 2008 Dynamics of quantum noise in a tunnel junction under ac excitation *Phys. Rev. Lett.* **100** 026601
[47] Basset J, Bouchiat H and Deblock R 2010 Emission and absorption quantum noise measurement with an on-chip resonant circuit *Phys. Rev. Lett.* **105** 166801
[48] Dubois J, Jullien T, Grenier C, Degiovanni P, Roulleau P and Glattli D C 2013 Integer and fractional charge Lorentzian voltage pulses analyzed in the framework of photon-assisted shot noise *Phys. Rev.* B **88** 085301
[49] Dmytruk O, Trif M and Simon P 2015 Cavity quantum electrodynamics with mesoscopic topological superconductors (arXiv:1502.03082)
[50] Qassemi F, Grimsmo A L, Reulet B and Blais A 2015 Quantum optics theory of electronic noise in coherent conductors (arXiv:1507.00322)
[51] Gabelli J and Reulet B 2013 Shaping a time-dependent excitation to minimize the shot noise in a tunnel junction *Phys. Rev.* B **87** 075403
[52] Gullans M J, Liu Y-Y, Stehlik J, Petta J R and Taylor J M 2015 Phonon-assisted gain in a semiconductor double quantum dot maser *Phys. Rev. Lett.* **114** 196802
[53] Rothstein E A, Entin-Wohlman O and Aharony A 2009 Noise spectra of a biased quantum dot *Phys. Rev.* B **79** 075307
[54] Levitov L S, Lee H and Lesovik G B 1996 Electron counting statistics and coherent states of electric current *J. Math. Phys.* **37** 4845–66
[55] Ivanov D A, Lee H W and Levitov L S 1997 Coherent states of alternating current *Phys. Rev.* B **56** 6839–50
[56] Dubois J, Jullien T, Portier F, Roche P, Cavanna A, Jin Y, Wegscheider W, Roulleau P and Glattli D C 2013 Minimal-excitation states for electron quantum optics using Levitons *Nature* **502** 659–63
[57] Jullien T, Roulleau P, Roche B, Cavanna A, Jin Y and Glattli D C 2014 Quantum tomography of an electron *Nature* **514** 603–7
[58] Murch K W, Weber S J, Beck K M, Ginossar E and Siddiqi I 2013 Reduction of the radiative decay of atomic coherence in squeezed vacuum *Nature* **499** 62–5

[59] Clerk A A, Devoret M H, Girvin S M, Marquardt F and Schoelkopf R J 2010 Introduction to quantum noise, measurement, and amplification *Rev. Mod. Phys.* **82** 1155
[60] Parlavecchio O, Altimiras C, Souquet J-R, Simon P, Safi I, Joyez P, Vion D, Roche P, Esteve D and Portier F 2015 Fluctuation–dissipation relations of a tunnel junction driven by a quantum circuit *Phys. Rev. Lett.* **114** 126801
[61] Torre E G D, Diehl S, Lukin M D, Sachdev S and Strack P 2013 Keldysh approach for nonequilibrium phase transitions in quantum optics: beyond the Dicke model in optical cavities *Phys. Rev.* A **87** 023831
[62] Clerk A A 2004 Quantum-limited position detection and amplification: a linear response perspective *Phys. Rev.* B **70** 245306
[63] Kamenev A 2011 *Field Theory of Non-Equilibrium Systems* (Cambridge: Cambridge University Press)
[64] Pedersen M H and Büttiker M 1998 Scattering theory of photon-assisted electron transport *Phys. Rev.* B **58** 12993–3006